MIT Open Access Articles

ON RELATIVISTIC DISK SPECTROSCOPY IN COMPACT OBJECTS WITH X-RAY CCD CAMERAS

Massachusetts Institute of Technology

ON RELATIVISTIC DISK SPECTROSCOPY IN COMPACT OBJECTS WITH X-RAY CCD CAMERAS

J. M. Miller[1], A. D'Aì[2], M. W. Bautz[3], S. Bhattacharyya[4], D. N. Burrows[5], E. M. Cackett[1], A. C. Fabian[6],
M. J. Freyberg[7], F. Haberl[7], J. Kennea[5], M. A. Nowak[3], R. C. Reis[6], T. E. Strohmayer[8], and M. Tsujimoto[9]

[1] Department of Astronomy, University of Michigan, 500 Church Street, Ann Arbor, MI 48109, USA; jonmm@umich.edu
[2] Dipartimento di Scienze Fisiche ed Astronomiche, Universita di Palermo, Palermo, Italy
[3] Kavli Institute for Astrophysics and Space Research, MIT, 77 Massachusetts Avenue, Cambridge, MA 02139, USA
[4] Department of Astronomy and Astrophysics, Tata Institute of Fundamental Research, Mumbai 400005, India
[5] Department of Astronomy & Astrophysics, Pennsylvania State University, 525 Davey Lab, College Park, PA 16802, USA
[6] Institute of Astronomy, University of Cambridge, Madingley Road, Cambridge, CB3 0HA, UK
[7] Max-Planck-Institut für extraterrestrische Physik, Giessenbachstraße, 85748 Garching, Germany
[8] Astrophysics Science Division, NASA Goddard Space Flight Center, Greenbelt, MD 20771, USA
[9] Japan Aerospace Exploration Agency, Institute of Space and Astronomical Sciences, 3-1-1 Yoshino-dai, Sagamihara, Kanagawa 229-8510, Japan

ABSTRACT

X-ray charge-coupled devices (CCDs) are the workhorse detectors of modern X-ray astronomy. Typically covering the 0.3–10.0 keV energy range, CCDs are able to detect photoelectric absorption edges and K shell lines from most abundant metals. New CCDs also offer resolutions of 30–50 ($E/\Delta E$), which is sufficient to detect lines in hot plasmas and to resolve many lines shaped by dynamical processes in accretion flows. The spectral capabilities of X-ray CCDs have been particularly important in detecting relativistic emission lines from the inner disks around accreting neutron stars and black holes. One drawback of X-ray CCDs is that spectra can be distorted by photon "pile-up," wherein two or more photons may be registered as a single event during one frame time. We have conducted a large number of simulations using a statistical model of photon pile-up to assess its impacts on relativistic disk line and continuum spectra from stellar-mass black holes and neutron stars. The simulations cover the range of current X-ray CCD spectrometers and operational modes typically used to observe neutron stars and black holes in X-ray binaries. Our results suggest that severe photon pile-up acts to falsely narrow emission lines, leading to falsely large disk radii and falsely low spin values. In contrast, our simulations suggest that disk continua affected by severe pile-up are measured to have falsely low flux values, leading to falsely small radii and falsely high spin values. The results of these simulations and existing data appear to suggest that relativistic disk spectroscopy is generally robust against pile-up when this effect is modest.

Key words: accretion, accretion disks – black hole physics – instrumentation: spectrographs – methods: analytical – X-rays: binaries

Online-only material: color figures

1. INTRODUCTION

X-ray observations of accreting neutron stars and black holes necessarily probe regions close to the compact object. The long-held promise of these observations is that aspects of the compact object itself, and the innermost accretion flow, may be revealed. Notable early attempts to realize this promise took several forms. For instance, many attempts were made to use the blackbody spectra of Type-I X-ray bursts in accreting neutron star systems to infer the stellar radius; however, derived radii were implausibly small, likely due to scattering effects (see London et al. 1986). In the case of black holes, careful efforts to measure the inner radius of the accretion disk (see, e.g., Makishima et al. 1986) were similarly complicated by various observational uncertainties such as mass and distance, and also by scattering effects (Shimura & Takahara 1995; Merloni et al. 2000).

At the most basic level, measurements of stellar or disk radii using blackbody or modified blackbody continua amount to counting photons under a curve to measure an absolute flux. This is extremely difficult (though not impossible) and easily complicated by additional continuum components and detector flux calibration uncertainties. Partially owing to difficulties associated with continuum spectroscopy, and partially owing to the detection of broad, possibly relativistic Fe K emission lines

in Cygnus X-1 (Barr et al. 1985) and 4U 1543−475 (van der Woerd et al. 1989; also see Park et al. 2004), parallel efforts to measure fundamental parameters focused on line spectroscopy.

Theoretical line models for non-spinning (Schwarzschild; $a = 0$, where $a = cJ/GM^2$) black holes and maximal-spin (Kerr $a = 0.998$; Thorne et al. 1974) black holes have been calculated for some time (Fabian et al. 1989; Laor 1991). Self-consistent models for hard X-ray illumination of an accretion disk that could give rise to such emission lines also have a long history (e.g., George & Fabian 1991). These models predict that lines arising in the inner disk should have skewed, asymmetric shapes, including a strong blue wing that is enhanced by special relativistic beaming and a long red wing that arises through Doppler shifts and gravitational redshifts. Line shapes are very difficult to discern at the resolution afforded by gas proportional counter spectrometers (e.g., $E/\Delta E \simeq 6$). Confirmation of this line shape was first achieved in an *ASCA* observation of the Seyfert-1 galaxy MCG-6-30-15 (Tanaka et al. 1995). It was facilitated by the X-ray charge-coupled devices (CCDs) aboard the mission, which delivered a resolution of ~ 12 in the Fe K band. Relativistic iron lines are merely the most prominent part of the broadband response of an accretion disk to hard X-rays, known as the disk reflection spectrum (see, e.g., George & Fabian 1991; Magdziarz & Zdziarski 1995; Dovciak et al. 2004; Ross & Fabian 2005).

X-ray CCDs and relativistic spectroscopy of black holes and neutron stars are thus intimately linked. The advanced CCD spectrometers aboard *Chandra*, *XMM-Newton*, and *Suzaku* have confirmed relativistic lines in a number of Seyfert-1 spectra (for a review, see Miller 2007). Just as importantly, the ability of these spectrometers to handle high flux levels has made it possible to clearly detect asymmetric lines in the spectra of stellar-mass black holes, and to reject the possibility that broad lines are actually a collection of narrow lines (see, e.g., Miller et al. 2002). If the inner disk is assumed to be truncated at the innermost stable circular orbit (ISCO), which is set by the spin of the black hole (see Bardeen et al. 1972), relativistic lines can be used to infer black hole spin parameters. In a number of stellar-mass black holes, the lines observed are sufficiently broad that varying degrees of black hole spin may be required (e.g., Miller et al. 2002, 2004a, 2008; Reis et al. 2009; Hiemstra et al. 2010; for a self-consistent analysis of eight systems, see Miller et al. 2009b).

Very recently, X-ray CCD spectroscopy of transient and persistent neutron star X-ray binaries has revealed skewed, asymmetric disk lines in these systems (see, e.g., Bhattacharyya & Strohmayer 2007; Cackett et al. 2008, 2009a; Di Salvo et al. 2009; D'Aì et al. 2009; D'Aì et al. 2010; for a self-consistent analysis of 10 systems, see Cackett et al. 2010.) In these sources, relativistic disk lines can be exploited to constrain the radius of the star, since the stellar surface (if nothing else) must truncate the disk wherein the lines arise. The inner extent of the disk is also related to the Alfven radius, and so can provide a constraint on stellar magnetic fields. In the case of the relativistic line observed in the millisecond X-ray pulsar SAX J1808.4−3658 (Cackett et al. 2009a; Papitto et al. 2009), the resulting field limits are commensurate with those derived from X-ray timing (Cackett et al. 2009a).

New, parallel efforts to derive fundamental properties of compact objects and inner accretion flows have been fueled by new disk models. New prescriptions explicitly incorporate inner torque conditions, radiative transfer through the disk atmosphere, and even black hole spin parameters (Zimmerman et al. 2005; Li et al. 2005; Davis & Hubeny 2006). Using these models, black hole spin parameters have been constrained in a number of systems (see, e.g., McClintock et al. 2006; Shafee et al. 2006; also see Zhang et al. 1997). The improved low-energy range of X-ray CCD detectors (often extending down to 0.3 keV) relative to current gas detectors (coverage below ∼ 3 keV is not possible with *RXTE* nor *International Gamma-Ray Astrophysics Laboratory* (*INTEGRAL*)) allows for improved measurements of the disk flux, and enables observers to separate disk emission from line-of-sight absorption in the interstellar medium (though in many cases dispersive spectroscopy may be required for this purpose; Miller et al. 2009b). Thus, while the improved energy resolution of X-ray CCD spectrometers is not necessarily critical for continuum spectroscopy, their energy range and spectral resolution are beneficial.

While measuring the width of lines is often easier than measuring an absolute flux, it still requires an accurate characterization of the underlying continuum flux, and an accurate knowledge of how the spectrometer reacts to high flux levels. The latter issue is typically unimportant for gas proportional counter spectrometers, but it can be important for X-ray CCD spectrometers. Indeed, the reaction of X-ray CCDs is important for both forms of relativistic spectroscopy of compact objects: an instrumental failure to accurately record the flux level is problematic for disk continua, and distortions to the continuum shape and energy response are problematic for line spectroscopy. Photon pile-up occurs when two or more photons land within a detection cell within a single CCD frame time. This causes a degeneracy between detecting N photons with energy E_i and a single photon with energy of $\Sigma_i^N E_i$. Thus when pile-up occurs, energy and flux information are lost.

It has recently been suggested that ineffective pile-up mitigation could produce spurious results concerning black hole spin, neutron star radii, and the radial extent of accretion disks as a function of the mass accretion rate (e.g., Yamada et al. 2009; Done & Diaz Trigo 2010; Ng et al. 2010). Advanced statistical descriptions of photon pile-up in X-ray CCD detectors have been developed (Davis 2001; also see Ballet 1999), and implemented into fitting packages such as XSPEC and ISIS. The Davis (2001) model has been applied in a number of regimes to correct for photon pile-up distortions, including spectra from: isolated neutron stars (e.g., van Kerkwijk et al. 2004), ultra-luminous X-ray sources (e.g., Roberts et al. 2004), transient Galactic black hole candidates (e.g., Jonker et al. 2004), low-mass X-ray binaries (e.g., Heinke et al. 2006), and even active galactic nuclei (AGNs; e.g., Wang et al. 2010). Most notably, Nowak et al. (2008) employed the basic elements of the Davis model to correct distortions to the *Chandra* spectra of the black hole candidate 4U 1957 + 11. Inner disk parameters consistent with those derived using spectra from other missions, including *XMM-Newton* and *RXTE*, were then recovered. A similar treatment of *Chandra* spectra of Cygnus X-1 by Hanke et al. (2009) was able to bring different spectra into close agreement.

With the aim of developing a rigorous understanding of how pile-up may affect relativistic spectroscopy, we have conducted extensive simulations based on a range of assumed input spectra, flux levels, and detector properties. This effort is timely as X-ray CCD spectrometers will be the standard in the field for the foreseeable future, at least for moderate resolution spectroscopy of bright targets. In the following sections, we briefly review the operation of X-ray CCD detectors, review the pile-up model used in our simulations, describe our simulations and results, and discuss the impacts of our findings.

The primary goal of this analysis is not to understand how to best avoid photon pile-up, though the results offer some insights on this point. Rather, the goal of this exercise is to understand the nature and magnitude of distortions to relativistic disk parameters when photon pile-up is present but unknown to an observer, poorly quantified, or difficult to mitigate in a rigorous manner. In a subset of our simulated spectra, then, photon pile-up is quite severe. When faced with similar real data, an observer would likely be motivated to extract an annulus or to otherwise at least partially mitigate the effects of pile-up.

2. THE BASICS OF X-RAY CCD SPECTROMETERS

At the most basic level, a CCD is an array of coupled capacitors. When an incident photon interacts in the semiconductor substrate, electrons are liberated. The charge is collected and stored in pixels, and it can be transferred to neighboring pixels—and eventually into an amplifier and read-out system—by virtue of the coupling.

In many respects, the operation of X-ray CCDs is similar to that of optical CCDs. One important difference is that optical photons only liberate a small number of electrons (typically zero or one) in an interaction. X-ray photons have much more energy, of course, and liberate many electrons. Indeed, the number

of electrons liberated in an interaction is proportional to the energy of the incident X-ray. This fact means that X-ray CCDs are not merely imaging instruments, but medium-resolution spectrometers as well. The gas proportional counters aboard *RXTE* have an energy resolution of ~ 6; current X-ray CCDs (e.g., *Chandra*/ACIS) achieve an energy resolution of ~ 30 at 5.9 keV.

Most X-ray CCDs cover the 0.3–10.0 keV band. These limits are set by a combination of factors, including the efficiency of capturing and clocking charge clouds generated by low energy X-rays (this is partially set by the electrodes), the depletion layer thickness, the ability of current X-ray mirrors to focus hard X-rays, and the ability of the instrument to distinguish hard X-rays from non-X-ray events. The detailed performance characteristics of a given X-ray CCD depend on several variables, including the nature of the device structure (n- or p-substrate, MOS or pn junction): whether charge is stored and read-out close to the X-ray-illuminated face of the CCD, or far from the illuminated face; the temperature at which the CCD is being operated (this affects dark currents and noise), and a number of more subtle factors.

Photons are detected and elementary screening of desirable (e.g., X-ray) versus undesirable (e.g., cosmic ray) events is achieved in part by assigning event "grades." Interactions are characterized using event "boxes," which are usually 3×3 cells of pixels. The pattern of pulse heights that are consistent with photon interactions can be defined and differentiated from "hot" pixel and cosmic ray patterns.

Efficient spectroscopy with an X-ray CCD depends on each event box recording zero or one photons per CCD frame time. When the X-ray flux incident on a CCD is too high, multiple photons can be read as a single high-energy photon (see above). The resulting flux is thus registered as falsely low, and the resulting spectrum as falsely hard. Grade migration provides a potential means of recognizing and diagnosing the degree of photon pile-up suffered in a given observation. When pile-up is important, charge patterns consistent with single photon interactions are reduced and patterns consistent with higher energy photon interactions or multiple photon interactions are increased.

Various strategies can be deployed to deliver nominal spectroscopic response even at high X-ray flux levels. The nominal CCD frame time can be greatly reduced, thus lowering the probability of two photons registering in a given event box. This often comes at the expense of imaging information, observing efficiency, or both. Over-sampling a broad telescope point-spread function (PSF) with a high number of event boxes is another viable means of limiting the number of photons that may land in a given event box. The expense of a broad PSF is, of course, the loss of fine image quality. Observers can try to further prevent or limit photon pile-up by only extracting events from the wings of the PSF in annuli, by placing a source-off of the optical axis of the telescope to blur its flux over more pixels, or by adopting a rigid grade selection that permits only single-photon events. In practice, however, some spectra obtained with X-ray CCDs will suffer from photon pile-up.

3. THE DAVIS PHOTON PILE-UP MODEL

Pile-up is a complex but well-understood statistical process: at a given flux level, a given event box has a fixed probability of getting 0, 1, or N photons. The probability of a given event grade for each outcome is also well determined. If the input spectrum is known, or if it can be estimated, the distribution of "good" event grades (those likely to originate from actual X-ray photons) can be used to infer the extent and severity of photon pile-up. On this basis, Davis (2001) has developed a model of photon pile-up. The model not only accounts for the energy shifts due to photon pile-up, but also for flux decrements due to grade migration.

The crux of the Davis model is a new integral equation for the number of counts detected from a point source. The conventional equation for the number of counts detected in an X-ray spectrometer is linear, and discussed in detail in Gorenstein et al. (1968). However, pile-up is a nonlinear process, and requires a more advanced treatment. Davis (2001) presents an alternative integral equation that accurately characterizes the counts observed in the presence of photon pile-up. A fundamental assumption of the pile-up model is that a charge cloud in the CCD arising from N photons can be treated as the linear superposition of N individual charge clouds. Since the drift time for charge clouds in a CCD is typically much less than a microsecond, which is much smaller than typical readout times, and since a CCD amplifier is highly linear at X-ray signal levels, this assumption is valid for all of the CCD modes that will be considered in this work.

In practice, the chief uncertainty in correcting for pile-up using this model is that the details of the input spectrum are usually not known a priori. Exceptions might include instances where different missions are simultaneously observing the same source, or an instance wherein a given CCD spectrometer alternates between different operational modes. This uncertainty does not enter into our analysis. Simulating the effects of photon pile-up by convolving different input spectra with the pile-up model of Davis (2001) is a well-controlled experiment—the nature of the input spectrum is known perfectly. The results of this procedure can be thought of as characterizing the nature and severity of systematic errors on relativistic disk parameters arising due to photon pile-up.

It is worth noting that although the pile-up model was developed for *Chandra*, it is easily applicable to other missions. The crucial modification in describing pile-up in other CCD spectrometers is to accurately account for the fraction of the telescope PSF that is enclosed in each event box. This can differ considerably from mission to mission. Whereas a single event box captures a high fraction of *Chandra's* PSF, a single event box captures a very small fraction of *Suzaku's* PSF. In the latter case, to evaluate pile-up in a reasonable extraction region, many event boxes must be considered jointly.

As implemented in the XSPEC spectral fitting package (Arnaud 1996), the Davis pile-up model has six parameters: the CCD frame time, the maximum number of photons to pile-up, the grade correction for a single photon, the grade morphing parameter (the grade migration function is a probability assumed to be proportional to α^{p-1}, $0 \leqslant \alpha \leqslant 1$, where α is the grade morphing parameter and p is the number of piled photons), the PSF fraction considered, and the number of event regions. This description of grade migration is based on the premise that photon arrival times in a given cell obey Poisson statistics. It correctly captures the fact that the probability of recording an unwanted event grade increases with the number of piled photons.

4. THE SIMULATED SPECTRA

To understand the specific effects of photon pile-up on disk continua and reflection parameters, we created a large number (325) of simulated spectra using the Davis pile-up model.

Realistic, multi-component spectral forms based on published results were employed to make the simulations as realistic as possible. The spectra were generated using the "fakeit" command in XSPEC version 12. For simplicity, and because this exercise is necessarily concerned with bright sources, no backgrounds were used in making the source spectra. In all cases, an exposure time of 100,000 s was used when creating simulated spectra. This exposure is longer than a typical observation, but allows for excellent photon statistics.

In all of the simulations made in this work, default values were assumed for the maximum number of photons to pile-up (5) and the grade correction for a single photon (1). The frame time, PSF fraction, and number of event boxes were set according to the telescope and CCD combination used in each simulation. With these parameters fixed, the grade morphing parameter α effectively sets the severity of photon pile-up (when the incident source flux in each event box leads to pile-up).

As implemented in XSPEC, the pile-up model is a convolution model. Input spectra were convolved with the pile-up kernel to produce a resultant spectrum that is distorted by photon pile-up effects. In practice, for a given detector and mode, the degree of pile-up is set by the incident flux level. In our simulations, the degree of photon pile-up was controlled by adjusting the grade morphing parameter α. Steps of 0.1 were used for $0.1 \leqslant \alpha \leqslant 0.8$, and steps of 0.04 were used for $0.8 \leqslant \alpha \leqslant 0.99$. The step size was reduced for high values of α in order to provide better resolution when pile-up typically starts to introduce strong distortions. For each combination of input spectrum and detector mode, then, 13 simulated spectra were generated.

5. INPUT SPECTRAL FORMS

X-ray binaries display a wide variety of phenomena. Periods of correlated multi-wavelength behaviors can be classified into "states" that may correspond to distinct changes in the accretion flow (for a review, see, e.g., Remillard & McClintock 2006; also see Belloni et al. 2005). In this work, we consider three commonly recognized "states" for black hole X-ray binaries, and a single input spectral form for neutron star low-mass X-ray binaries (the so-called Z and atoll sources). In the interest of simplicity and reproducibility, we have adopted phenomenological spectral models for each state with values consistent with those reported in the literature. Table 1 lists values for all of the input spectra considered in this work. The paragraphs below offer some context and motivation for why certain models and values were used to generate the spectra.

The very high state. This state can be extremely bright and it has seldom been observed using CCD spectrometers. Continua observed in this state often consist of a hot disk and steep power-law component. We assumed the continuum parameters measured in the very high state of GX 339−4 using the *XMM-Newton*/EPIC-pn in "burst" mode (Miller et al. 2004a). This mode has a frame time of just 7 μs and a deadtime of 97%, but it is effective at preventing photon pile-up for fluxes up to 6 Crab. The particular spectrum chosen as a template is broadly consistent with very high state spectra obtained from *RXTE* monitoring of other transients (e.g., 4U 1543−475, Park et al. 2004; GRO J1655−40, Sobczak et al. 1999; XTE J1550−564, Sobczak et al. 2000; Miller et al. 2003).

The "intermediate" state is similar to the "very high" state in terms of its spectral form (both thermal disk and non-thermal power-law-like emission are important), but typically has a

Table 1
Input Model Parameters

Parameter	Very High/Intm.	Low/Hard	High/Soft	Z/Atoll
$N_{\rm H}(10^{22}\rm cm^{-2})$	0.5	0.5	0.5	0.5
$kT_{\rm disk}$ (keV)	0.76	0.18	0.97	1.21
$K_{\rm disk}$	2300.0	160000.0	7050.0	103.0
$kT_{\rm bbody}$ (keV)	$\cdots$	$\cdots$	$\cdots$	2.28
$K_{\rm bbody}$ (10^{-2})	$\cdots$	$\cdots$	$\cdots$	4.9
Γ	2.60	1.60	2.48	3.60
$K_{\rm pl}$	2.20	0.50	3.38	0.18
$E_{\rm Laor}$ (keV)	6.7	6.7	$\cdots$	6.7
q	3.0	3.0	$\cdots$	3.0
$r_{\rm in}(GM/c^2)$	6.0	6.0	$\cdots$	6.0
i (deg)	30.0	30.0	$\cdots$	30.0
$K_{\rm line}(10^{-3})$	7.7	8.5	$\cdots$	8.0
Flux $(10^{-9}\rm ergcm^{-2}s^{-1})$	36.9	2.9	86.2	6.0

Notes. The table above lists the input spectral parameters used to generate the simulations considered in this work. The spectral parameters were chosen to be representative of different spectral states in stellar-mass Galactic black holes, and a typical medium-intensity state in an "atoll" neutron star X-ray binary. The "very high" or "intermediate" state parameters are based on an observation of GX 339−4 as reported by Miller et al. (2004a); the "low/hard" state parameters are based on observations of GX 339−4 as reported by Miller et al. (2006), Tomsick et al. (2008), and Wilkinson & Uttley (2009); the "high/soft" state parameters are taken from an observation of 4U 1543−475 made on MJD 52452 as reported by Park et al. (2004), and the typical Z/Atoll spectrum is based on an observation of Serpens X-1 from Cackett et al. (2008). In the case of the neutron star spectrum, three continuum components (a disk blackbody, a simple blackbody, and a power-law) are needed to model the continuum. The observed (absorbed) flux is given for each input spectrum.

lower flux. The effects of photon pile-up in this state are likely to be similar to the effects on very high state spectra at low values of the grade migration parameter α. The "intermediate" state is not treated separately in this work.

The high/soft state. This state can also be quite bright, but it typically persists for a longer period than the "very high state." As a result, it is more commonly observed with CCD spectrometers. Continua observed in this state are strongly dominated by a hot disk component, accompanied by a weak, steep power law. To model the high/soft state, we selected one of the spectrally softest observations of 4U 1543−475 obtained using *RXTE* (Park et al. 2004). This observation occurred on MJD 52475, and is consistent with the spectra selected for relativistic disk spectroscopy by Shafee et al. (2006). Here again, this high/soft state is typical of spectra of other black hole transients in the same state (see, e.g., Sobczak et al. 1999, 2000).

The low/hard state. The low/hard state has been a frequent target with CCD spectrometers recently, in an effort to understand the accretion flow at low-mass accretion rates (for a recent survey, see Reis et al. 2010; also see Tomsick et al. 2009). Spectral continua in this state are dominated by a hard power law, sometimes with weak emission from the accretion disk. The continuum spectrum assumed in our simulations is a composite of the parameters reported in observations of GX 339−4 by Miller et al. (2006), Tomsick et al. (2008), and Wilkinson & Uttley (2009).

A typical Z/atoll spectrum. Unlike most black hole X-ray binaries with low-mass companions, neutron stars with low magnetic fields are typically persistent (but variable) sources. Whereas black hole continua can often be well characterized in terms of thermal disk emission and a power law, neutron star spectra often require a third component (Lin et al. 2007;

Cackett et al. 2008; Cackett et al. 2010; D'Aì et al. 2010). A simple blackbody likely corresponds to emission from the boundary layer between the accretion disk and stellar surface (Revnivtsev & Gilfanov 2006). Emission from this region may be Comptonized, but blackbody emission that is Compton upscattered in a region with high τ and low kT_e can be modeled with a hotter, smaller blackbody (London et al. 1986). We used the spectral continuum parameters reported by Cackett et al. (2008) for Serpens X-1.

5.1. Relativistic Line Properties

Relativistic line components were added to all continuum spectra, apart from those for the "high/soft" state. The "Laor" relativistic emission line model (Laor 1991) was assumed to simulate emission lines from the inner disk. In all cases, the input inner radius was fixed at $6GM/c^2$, the emissivity index was fixed at $q = 3$ (where $J(r) \propto r^{-q}$), and the inclination was fixed at $30°$. This radius is substantially larger than the innermost stable circular orbit for a maximally spinning Kerr black hole ($1.24GM/c^2$) and significantly larger than measured in a number of stellar-mass black holes (Miller et al. 2009b). However, one purpose of this investigation is to see if photon pile-up can artificially *broaden* relativistic lines, giving falsely small inner radii and falsely high spin values. Setting the inner radius at $6GM/c^2$, then, permits distortions due to photon pile-up ample opportunity to produce falsely broad lines. For all simulated black hole spectra, the input flux of the relativistic "Laor" line was normalized to give an equivalent width of 300 eV as per Miller et al. (2004a).

Similarly, $6GM/c^2$ is approximately 12.4 km for a 1.4 $M_\odot$ neutron star—only slightly larger than the canonical stellar radius of 10 km employed in many circumstances. Assuming the stellar surface (if not the boundary layer) must truncate the accretion disk, a relativistic line suggesting a smaller radius might be taken as evidence of a "strange" star. In the case of neutron stars, then, fixing the input radius at $6GM/c^2$ serves to assess the ability of photon pile-up to give false evidence of "strange" stars through falsely small disk radii. For all simulated neutron star spectra, the input flux of the "Laor" line was normalized to given an equivalent width of 150 eV as per Cackett et al. (2008).

Iron emission lines in accreting black holes and neutron stars are merely the most prominent part of the disk reflection spectrum (e.g., Dovciak et al. 2004; Ross & Fabian 2005). Self-consistent modeling of real spectra requires modeling of the entire reflection spectrum, not just the broadened emission line. For simplicity, and because the line drives constraints on inner disk radii (and therefore spin) in fits to real data, disk reflection models are not treated in this analysis.

5.2. The Thermal Disk Continuum

In all spectra, thermal continuum emission from the accretion disk was simulated using the simple "diskbb" model (Mitsuda et al. 1984) within XSPEC. Using this model, the inner disk radius can be derived via: $r = (d/10\text{kpc}) \times (K/\cos\theta)^{1/2}$km, where K is the model flux normalization, d is the distance to the source, and θ is the inclination of the inner disk. If the mass of the source is known, this radius can be converted to gravitational units.

This is merely a "color" radius, however, and does not account for the effects of spectral hardening due to radiative transfer through the disk atmosphere (Shimura & Takahara

1995; Merloni et al. 2000). It is well known that this model is overly simple in other ways. For instance, it does not include a zero-torque condition at the inner edge, whereas including this condition can reduce implied radii by a factor of ~ 2 (Zimmerman et al. 2005). Moreover, a number of new disk models have been developed in which black hole spin is an explicit parameter (Davis & Hubeny 2006).

Deriving spins using these newer, more physical models requires extremely accurate knowledge of the absolute disk flux, however, which can be complicated by a number of effects (e.g., the flux calibration of the detector, the accuracy to which line of sight absorption is known, the nature of the hard component, etc.). And whereas new models can have as many as 10 free parameters, the "diskbb" model is able to accurately characterize the thermal continuum with only two (temperature and flux normalization). Owing to its simplicity and prior application to many neutron star and black hole spectra over numerous years and X-ray missions, then, all thermal disk continua were simulated using the "diskbb" model, and our analysis is primarily concerned with changes in the flux normalization parameter.

In the Z/atoll spectra, a simple (single-temperature) black-body function was used to describe emission from the stellar surface, independent of the thermal emission from the disk.

5.3. Interstellar Absorption

Each input spectrum was modified by interstellar absorption using the "tbabs" model (Wilms et al. 2000). In all cases, the equivalent neutral hydrogen column density was fixed at $N_H = 5.0 \times 10^{21}$cm^{-2}. This is a moderate value, consistent with columns that have facilitated studies of the thermal disk continuum in a number of sources and at different mass accretion rates.

5.4. Simulations with Gaussian Lines

Although a number of observations made with the *Chandra*/HETGS (e.g., Di Salvo et al. 2005) and with *Suzaku* (Cackett et al. 2008; Reis et al. 2009; Cackett et al. 2010) find broad, relativistic line shapes in the spectra of neutron stars, such lines are less established in neutron star spectra than in black hole spectra. Ng et al. (2010) suggest that neutron star lines may actually be narrower ($\sigma = 0.33$ keV, on average) and symmetric. Therefore, we also simulated neutron star spectra using the same neutron star continuum described above and in Table 1, but with a Gaussian model with $E = 6.7$ keV, $\sigma = 0.33$ keV, and an equivalent width of 150 eV, rather than a relativistic line.

6. DETECTORS AND MODES

The CCD spectrometers and modes considered in our simulations are detailed in Table 2. The modes selected reflect those that users might realistically select when observing bright sources. The "burst" mode of the EPIC-pn camera aboard *XMM-Newton* is not considered, as it is capable of handling exceptionally high flux levels without pile-up distortions. Common imaging modes available on the ACIS and X-ray Telescope (XRT) instruments aboard *Chandra* and *Swift*, respectively, are also not considered; these are known to readily suffer pile-up for even moderately bright sources and are typically avoided by users. Finally, with *Chandra*, pile-up can be largely mitigated while obtaining a high-resolution spectrum with the HETGS; however, assessing pile-up in this circumstance is especially complex and beyond the scope of this investigation.

Table 2
Detectors, Modes, and Parameters

Mission/Instrument & Mode	T_R^a (10^{-3} s)	Radius[b] (arcsec)	Pixel Size[c] (arcsec)	Event Box[d] (pixels)	$T_{\rm eff.}^e$ (10^{-3} s)	Regions[f]
Chanda/ACIS "continuous clocking"	2.85	2.5	0.5	3×3	8.55	3.3
Swift/XRT "windowed timing"	1.77	9.0	2.36	10 × 7	1.77	1.1
XMM-Newton/pn "timing"	0.03	120	4.1	30 × 3	0.09	1.0
XMM-Newton/MOS "full frame"	2600	20	1.1	3×3	2600	115.3
Suzaku/XIS "1/4 Window+0.3 s Burst"	300	60.0	1.0	3×3	300.0	1256.0

Notes. The table above lists important features of the detectors and modes considered in our simulations, as well as the details of the extraction regions that were assumed. Please see Section 6 for a detailed discussion.

[a] T_R is the time resolution of a given instrument and mode. In standard imaging modes, this is the "frame time" over which the CCD records data. In specialized timing modes, T_R is actually the time to transfer one row (of pixels or macropixels) of charge.

[b] This column gives the "radius" of the extraction regions used in simulating an observation using a given detector and mode. For *Chandra*, the PSF is sufficiently small that the 90% encircled energy radius was used. For other missions, nominal extraction regions were selected to reflect the radius over which the encircled energy changes approximately linearly with radius. In the case of *Suzaku* and *Swift*, the radii used are essentially the half-power radii. The radii used for the *XMM-Newton* MOS and pn cameras encircle approximately 70% and 75% of the total incident energy, respectively.

[c] This column gives the nominal pixel size for each detector.

[d] This column gives the size of an event box for each detector and mode considered. The *Suzaku* mode and *XMM-Newton*/EPIC-MOS modes considered in this work are imaging modes wherein standard pixels and event boxes are retained. The *Chandra*/ACIS "continuous clocking" mode is a specialized timing mode but retains the standard 3×3 event box used in imaging modes. The *XMM-Newton*/EPIC-pn "timing" and *Swift*/XRT "windowed timing" modes achieve a fast read-out partially by creating "macropixels" that are 30 pixels and 10 pixels, respectively, in the read-out direction. The *Swift* "windowed timing" mode is unique in that the event box is changed from a 3×3 format to a 10 × 7 format.

[e] $T_{\rm eff}$ is the effective time resolution for a given instrument and mode. In specialized timing modes, this is the time to clock one full event box of charge, not merely one row of charge.

[f] This field notes the number of event boxes that cover the extraction radius.

An "effective" frame time is given in Table 2. This is the frame time that is important to consider when assessing the extent and impacts of photon pile-up. It multiplies the time required to extract one element of charge (typically a pixel, but sometimes a larger "macropixel") by the number of elements necessary to define an event box. (Some missions—but not all—redefine event boxes for different modes; see the discussion below.) If one could know a priori that a sequence of events were all "singles" wherein charge from photon events was contained in only one pixel, then the effective frame time would equal the time required to clock just one row of pixels. However, it is not possible to know this a priori, and in practice one only knows that an event was a "single" if the other rows in an event box are free of charge. Thus, for pile-up, the timescale of concern is the time required to transfer a full event box.

A significant simplification in our simulations is that the grade morphing parameter α is assumed to be constant in each extraction region. In practice, this is not true; α would depend on radius as an actual telescope PSF focuses successively less energy into successively larger annuli. Our simulations, therefore, capture the strongest impacts of photon pile-up distortions and ignore how less distorted spectra from large annuli might affect results when summed with spectra from smaller annuli. In a partial effort to minimize the impact of the assumption of a constant α, the extraction regions assumed in our simulations do not encircle the same fraction of the total incident energy, but rather attempt to sample the part of the PSF where the encircled energy changes only linearly with radius. This is not practical in the case of *Chandra*, however, which has a very tight PSF. A secondary simplification is that the pile-up model and our simulations do not consider how charge from event boxes might bleed into adjacent boxes in the case of severe pile-up.

Additional details concerning the individual spectrometers and modes considered, and how they are treated in our simulations, are given below.

6.1. Chandra/ACIS Continuous Clocking Mode

ACIS event boxes consist of a 3×3 box of pixels, each approximately 0.5″ on a side. In continuous clocking or "CC" mode, charge is continuously transferred from the CCD (usually ACIS-S3) at a rate of 2.85 ms per row. Two-dimensional imaging is sacrificed in favor of fast read-out. The definition of ACIS event boxes is unchanged between standard imaging modes and CC mode. In our simulations, then, we have assumed an effective frame time of 8.55 ms, since this is the time required to clock a full event box.

As noted above, given the tight PSF of *Chandra*, it is impractical to extract photons from a region that encircles less than 90% of the incident energy. In our simulations, we therefore assumed an extraction radius of 2″.5, which corresponds to 90% of the incident energy. In the one-dimensional regime of CC mode, the extraction region is then a bar 5″ in length. Note that this means that only 3.3 event boxes tile the extraction region.

Where possible, generic, readily available response matrices were used in order to facilitate checks on this work by other teams. To simulate ACIS CC mode spectra, then, we used the ACIS response matrices made available by the mission for simulations supporting Cycle 11 proposals: "aciss_aimpt_cy11.rmf" and "aciss_aimpt_cy11.arf." For more information about the ACIS spectrometer and CC mode, please see Garmire et al. (2003) and the *Chandra* Proposer's Observatory Guide (http://cxc.harvard.edu/proposer/POG/).

6.2. Swift XRT Windowed Timing Mode

In "windowed timing" or "WT" mode, charge rows are grouped by 10 in the read-out direction (effectively creating "macropixels") and rapidly transferred from the CCD. In the standard photon counting mode, a 3×3 grouping of pixels (each pixel is 2″.36 on a side) is used to define an event box. However, in windowed timing mode, the event box is altered to be

10 × 7 pixels: 1 macropixel in the clocking direction, and 7 pixels in the orthogonal direction. This change improves the ability of the detector to identify and screen events in windowed timing mode. Note that because the new event box is only 1 macropixel in the clocking direction, the nominal and effective frame times are the same in windowed timing mode (see Table 2). Like *Chandra*/ACIS "continuous clocking" mode, "windowed timing" mode has a live-time fraction of 1.0.

In our simulations, we assumed an extraction radius of 9″.0, which roughly corresponds to the half-power radius for the *Swift*/XRT. The extraction region is tiled by only 1.1 event boxes. For simplicity, we have also assumed an effective frame time of 1.77 ms (see Table 2). In practice, depending on where a photon strikes, it may take up to two read-out times of 1.77 ms to clock the charge through the extraction region (which roughly matches the half-power diameter of the PSF). In this sense, our simulations slightly underestimate the severity of pile-up distortions to *Swift*/XRT spectra obtained in "windowed timing" mode.

To simulate "windowed timing" mode spectra, we used current, standardized response functions available through the HEASARC calibration database, "swxwt0to2s6_20070901v011.rmf" and "swxwt0to2s6_200101 01v011.arf." These responses have been developed specifically for WT mode, and differ from the responses appropriate for normal imaging modes.

For more information about the *Swift*/XRT, please see Hill et al. (2004), Burrows et al. (2005), the *Swift* Technical Handbook (http://swift.gsfc.nasa.gov/docs/swift/proposals/appendix_f. html) and the XRT User's Guide (http://swift.gsfc.nasa.gov/docs/swift/analysis/xrt_swguide_v1.2.pdf).

6.3. XMM-Newton EPIC-pn "Timing" Mode

The "timing" mode of the EPIC-pn camera is similar to the "windowed timing" mode of the *Swift*/XRT in some respects. To achieve a high time resolution, normal CCD pixels are grouped into "macropixels." Each macropixel is 10 pixels in the read-out direction and 1 pixel in the orthogonal direction. Since each pixel is 4″.1 on a side, this means that a single macropixel is actually 41″ in the read-out direction. In its long dimension, then, a single macropixel is equivalent to the 70% encircled energy diameter of the telescope. In standard imaging modes, *XMM-Newton* event boxes are the standard 3×3 pixel element, as per other X-ray CCD cameras. In timing mode, however, an event box is 3 macropixels by 3 macropixels. This means that a single event box is 123″ long (equivalent to the 95% encircled energy diameter) and 12″.3 wide (approximately equal to the half-power diameter). This event box is extremely large and roughly equivalent to the extraction region that is often used by observers using this mode.

Creating macropixels enables a short read-out time of 0.03 ms *per macropixel*. This translates to an effective frame time of 0.09 ms *per event box*. Again, this is a simplification that may serve to underestimate the severity of photon pile-up distortions to "timing" mode spectra. In practice, each macropixel takes at least three read-out times to be completely clocked, and it may take four timescales depending on where the photon strikes. Thus, each macropixel may contain more charge than anticipated in these simplified simulations.

The short frame time achieved in "timing" mode is impressive, especially considering that "timing" mode operates with a live-time fraction of 0.99. Unlike its cousin, "burst" mode (live-time fraction: 0.03), "timing" does not handle high fluxes

by making exceptionally short exposures while discarding the bulk of the incident flux. These abilities come at the expense of tiling the PSF with many event boxes, however, which is another important means of reducing the severity of photon pile-up distortions.

A distinctive feature of the *XMM-Newton*/EPIC-pn camera is that diagonally adjacent pixels are treated as two single pixel events. Differences between detectors at this level are assumed to be small.

Generic and separate redistribution and ancillary matrix files are not readily available to *XMM-Newton* users. Timing mode response matrices were generated using the "rmfgen" and "arfgen" tools in SAS version 9.0.0. These matrices were then used to simulate all timing mode spectra.

For more information about *XMM-Newton* and the EPIC-pn camera, please see Strüder et al. (2001), Haberl et al. (2004), and the User's Handbook (http://xmm.esac.esa.int/external/xmm_user_support/ documentation/index.shtml).

6.4. XMM-Newton EPIC MOS "Full Frame" Mode

"Full frame" mode is a standard imaging mode for the MOS 1 and MOS 2 cameras aboard *XMM-Newton*, not a specialized timing mode like those described above. There are two reasons for considering it in this analysis. First, the small, 1″.1 pixels of the MOS cameras allow for a large number of event boxes to tile an extraction region, which is one viable strategy for reducing the effects of photon pile-up. Second, by extracting annuli that excise central regions within a piled-up source image, observers are often able to make use of data obtained in this and similar operating modes. Whether or not pile-up is totally mitigated through this procedure is sometimes in doubt, and this analysis can help to clarify the nature of any distortions imposed on the extracted spectrum by residual pile-up.

In simulating MOS "full frame" spectra, circular extraction regions with 20″ radii were assumed. Within this range, the encircled energy fraction of the PSF changes almost linearly with radius. The regions assumed would encircle approximately 70% of the total incident energy. As with pn "timing" mode, responses were generated using the "rmfgen" and "arfgen" functions within SAS version 9.0. These responses were then used to create all simulated "full frame" spectra.

For additional information on the *XMM-Newton*/EPIC-MOS cameras, please see Turner et al. (2001).

6.5. Suzaku Windowed Burst Mode

The X-ray Imaging Spectrometer (XIS) aboard *Suzaku* provides many different operational modes that can be used to optimize science returns and to reduce or eliminate photon pile-up. Each XIS CCD has a nominal frame time of 8.0 s, but this can be reduced by choosing a "window" option. For instance, using a 1/4 window means that only 1/4 of the CCD will be exposed, reducing the frame time to 2.0 s. (Smaller windows are possible but cannot be used owing to drift in the spacecraft pointing over the course of an observation.) The frame time can be further reduced by selecting a "burst" option; in this case, the CCD only exposes for a fraction of the nominal frame time. The remainder of the frame time is then dead time, reducing the overall observing efficiency and requiring longer exposures. For this analysis, the second-most conservative combination of window and burst option has been considered. For all simulated spectra, we assumed a 1/4 window and 0.3 s burst option.

It should be noted that the XIS can be operated in "PSUM" mode, wherein the full height of the CCD is read-out in the time

normally required to clock one row of charge. In some respects, this mode is similar to the "timing" and "burst" modes available on the *XMM-Newton*/EPIC-pn camera, and for similar reasons it is actually less effective at mitigating pile-up than the most conservative combinations of XIS window and burst options.

Each simulated spectrum assumed a circular extraction region with a radius of $60''$, which encircles approximately half of the incident energy for the *Suzaku* PSF. Within this radius, the encircled energy fraction changes in a roughly linear way with radius. Each XIS pixel is $1''$ on a side, and standard 3 pixel by 3 pixel boxes are used to define event grades. Within the extraction region, then, there are 1256.0 event boxes. Tiling a broad PSF with many event boxes acts to reduce the flux per event box.

For more information on the XIS, see the *Suzaku* ABC Guide (http://heasarc.gsfc.nasa.gov/docs/suzaku/analysis/abc/) and the *Suzaku* Technical Description (http://heasarc.gsfc.nasa.gov/docs/suzaku/aehp_prop_tools.html).

7. ANALYSIS AND RESULTS

All simulated spectra were fit using the same model components that were employed to generate the spectrum, but without using the pile-up kernel. This procedure permits an examination of how spectral fitting results are distorted by photon pile-up effects, when such effects have not been mitigated entirely (e.g., by extracting events in an annulus, by selecting a shorter frame time, etc.). For the purpose of illustrating how parameters are distorted even in the event of severe photon pile-up, fits were made even when the χ^2 goodness-of-fit statistic was not acceptable. All errors reported in this analysis are 1σ confidence errors, and were determined using the "error" command within XSPEC. In the cases where the fits were unacceptable, the errors are not true 1σ errors.

A few simplifying assumptions were made in fitting the simulated spectra. The equivalent neutral hydrogen column density was held fixed at the input value, $N_H = 5.0 \times 10^{21} \text{cm}^{-2}$. In practice, this might be equivalent to assuming the column density measured via a sensitive *Chandra*/HETGS or *XMM-Newton*/RGS spectrum in which individual neutral photoelectric absorption edges were detected (e.g., Miller et al. 2009a). Some of the relativistic iron line parameters were constrained to ranges and/or fractional uncertainties that are common in the literature. Specifically, all fits to the simulated line spectra assumed $6.70\text{keV} \leqslant E \leqslant 6.97\text{keV}$, $3 \leqslant q \leqslant 5$, and $10° \leqslant \theta \leqslant 50°$. Fits to the simulated spectra were otherwise unconstrained; line and continuum model parameters were free to take on whatever value best described the distorted spectra.

The goal of this analysis is simply to understand how disk reflection and disk continua are affected by pile-up. A detailed treatment of distortions to (more physical) continuum spectra (e.g., Comptonization spectra, and/or coupled disk plus corona models such as "eqpair") might also be timely, but it is beyond the scope of this paper. The sections that follow are narrowly focused on the results of fits to relativistic lines and simple disk continua.

7.1. Pile-up and Relativistic Lines

The results of these limited exercises are clear: when photon pile-up is severe, it causes relativistic emission lines in black hole spectra to be measured as falsely narrow. In fits to the simulated spectra with the Laor line model, measured radii were all consistent with or significantly larger than the true value of
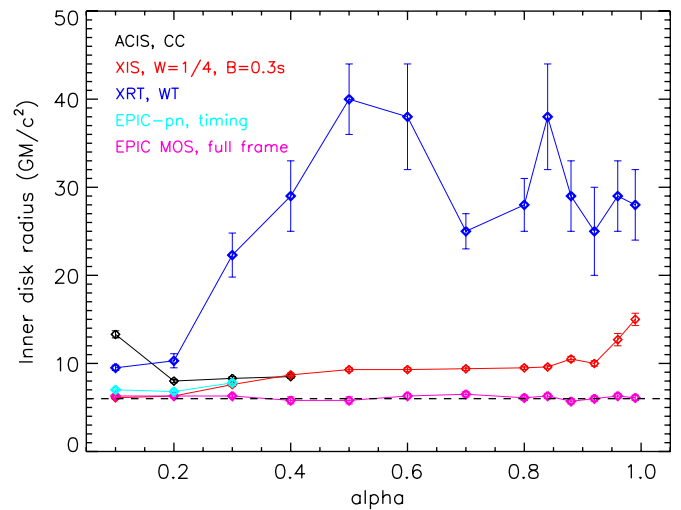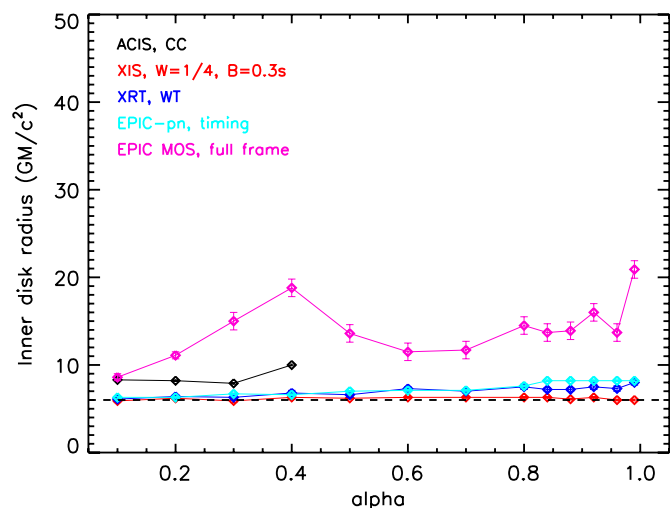

Figure 1. Plot above depicts the evolution of the inner disk radius measured via a relativistic iron emission line (in units of GM/c^2) vs. the severity of photon pile-up (governed by the grade migration parameter α), for simulated spectra assuming a form typical of the "very high" state in accreting black holes (see Section 5 and Table 1). The dashed horizontal line at $6GM/c^2$ denotes the input radius used in all simulated spectra. An iron line could not be required in fits to simulated *Chandra*/ACIS "continuous clocking" mode spectra past $\alpha = 0.92$, nor above $\alpha > 0.3$ for fits to simulated EPIC-pn spectra. Fits to simulated EPIC MOS spectra do not show an evolution in radius because pile-up is so severe that event loss dominates over grade migration distortions; this is a limitation of our simulations and it does not suggest that the MOS should be operated in "full frame" to observe a source this bright. The results above suggest that the *Suzaku*/XIS (with a 1/4 window and 0.3 s burst option) and *Swift*/XRT (in windowed timing mode) are capable of dealing with flux levels this high but would give falsely large disk radii unless pile-up distortions were mitigated (e.g., by extracting counts in annuli).

(A color version of this figure is available in the online journal.)

$6GM/c^2$. Figures 1 and 2 trace the evolution of measured radius as a function of pile-up severity (set by the grade migration parameter α). Figure 3 shows how the entire spectrum is affected by pile-up. Figure 4 shows a sequence of line profiles from simulations with increasing photon pile-up. The same results hold in the case of our simulated neutron star spectra, with one modest exception (see below).

Even the baseline flux level assumed in our "very high" state simulations (corresponding to low values of α) is found to completely overwhelm *Chandra*/ACIS "continuous clocking" mode and *XMM-Newton*/EPIC-pn "timing" mode. The emission line could not be detected nor reliably fit except at low values of the grade migration parameter α. In any real observation at an even higher flux level (corresponding to a higher value of α), then, a line may not be clearly detected. Similarly, for the *XMM-Newton*/EPIC MOS in "full frame" mode, event loss dominates over grade migration in the simulated spectra, and so the *shape* of the spectrum—including the line—is preserved though the line and continuum flux are a small fraction of their input values. The results shown in Figure 1 do not indicate that the MOS "full frame" mode is equipped to deal with typical "very high" state flux levels.

The *Swift*/XRT in "WT" mode and *Suzaku*/XIS (with 1/4 window and 0.3 s burst option) are less overwhelmed by the high flux associated with our baseline "very high" state spectrum. In fits to those simulated spectra, the inner disk radius correlates with the severity of pile-up as traced by the grade migration parameter α (again, α serves as a proxy for increasing the flux over the baseline levels given in Table 1). The results shown in Figure 1 indicate that the *Suzaku*/XIS is actually best equipped to deal with such high flux levels, although even in this case fits

Figure 2. Evolution of the inner disk radius measured via a relativistic iron emission line (in units of GM/c^2) vs. the severity of photon pile-up (governed by the grade migration parameter α), for simulated spectra assuming a form typical of the "low/hard" state in accreting black holes (see Section 5 and Table 1). The dashed horizontal line marks the input radius of $6\,GM/c^2$. An iron line could not be required in fits to simulated *Chandra*/ACIS "continuous clocking" mode spectra past $\alpha = 0.4$. The results shown above suggest that the *Suzaku*/XIS (with a 1/4 window and 0.3 s burst option) can potentially deliver a nearly nominal response and accurate radii at flux levels typical of the "low/hard" state. In contrast, our results suggest that radii derived from spectra obtained using other detectors and modes could be too high by approximately 30%, unless additional mitigations were adopted.

(A color version of this figure is available in the online journal.)
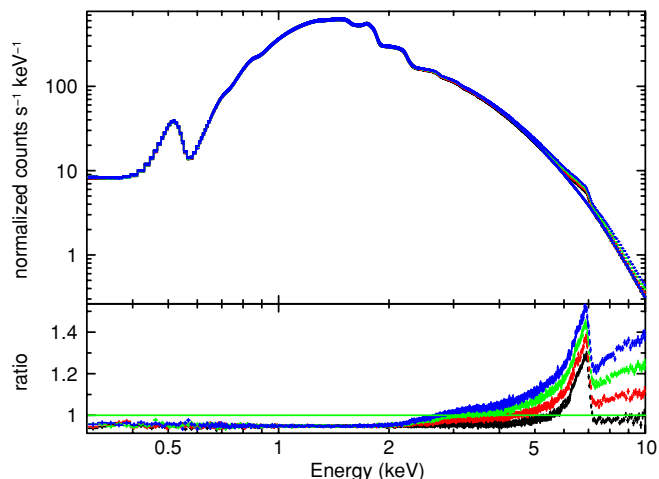
Figure 3. Illustration of the effect of pile-up on the spectral continuum. The spectra shown above were fit using the parameters of the input spectral model. In this case, simulated "very high" state inputs were used, and observations with the *Suzaku*/XIS responses assuming a 1/4 window option and 0.3 s burst option are shown. Values of the grade migration parameter $\alpha = 0.1, 0.4, 0.7, 0.96$ are shown above in black, red, green, and blue, respectively. As pile-up becomes more severe, the high-energy continuum becomes harder due to event grade migration.

(A color version of this figure is available in the online journal.)

to the iron line fail to recover the full line width and give falsely large inner disk radii. The apparent fluctuations in inner disk radius at high values of α seen in the XRT trend in Figure 1 are likely the result of errors that are underestimated because the overall fit is poor.

In the "low/hard" state, the degree of spectral distortions is generally reduced with respect to the "very high" state (see Figure 2). The most accurate inner disk radii were recovered in
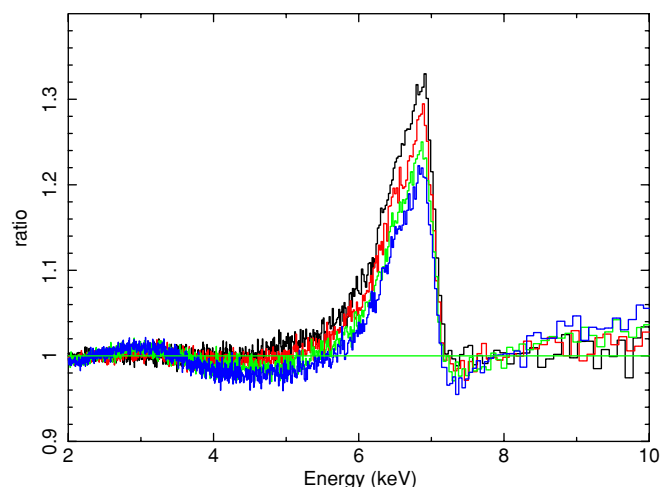
Figure 4. Illustration of the effect of pile-up on iron lines. As pile-up becomes more severe, an excess grows between 2 and 3 keV, a flux decrement can be seen between 3 keV and 5 keV, and the line becomes narrower. This is due to a combination of flux redistribution, grade migration, and event loss altering the shape of the continuum spectrum. The plot above was made by fitting simple disk plus power-law continua to simulated "very high/intermediate" state spectra using the *Suzaku* XIS responses and assuming a 1/4 window and 0.3 s burst option. The 4–7 keV region was ignored when fitting the continuum, and then included when making the data/model ratio plot shown above. Values of the grade migration parameter $\alpha = 0.1, 0.4, 0.7, 0.96$ are shown above in black, red, green, and blue, respectively. Errors have been neglected for visual clarity.

(A color version of this figure is available in the online journal.)

the simulated *Suzaku*/XIS spectra. A 1/4 window option and 0.3 s burst option appear to suffer minimal distortion due to photon pile-up, at least for the flux levels that would generate the values of α that were simulated. Photon pile-up distortions are more pronounced in the other spectra: measured inner disk radii are found to depart more strongly from the true value with increasing α. The *XMM-Newton*/EPIC-pn "timing" mode and *Swift*/XRT "windowed timing" mode appear to only suffer modest distortions as pile-up becomes more severe: in each case, lines are measured to be falsely narrow and to give inner disk radii that are too large by 2–3 GM/c^2. Fits to the simulated *XMM-Newton*/EPIC MOS spectra in "full frame" mode show the most marked trend: even for the lowest flux levels (lowest values of α), pile-up is so severe that measured inner radii depart from the input value by factors of a few. The *Chandra*/ACIS "continuous clocking" mode is still overwhelmed at the baseline flux level given in Table 2, and lines cannot be required in spectral fits for $\alpha > 0.4$.

As with the "low/hard" state, the simulated *Chandra*/ACIS "CC" mode neutron star spectra were severely distorted by photon pile-up, and other modes were less affected. It was only possible to detect and fit the iron line reliably for $\alpha = 0.1$ for *Chandra*/ACIS "continuous clocking" mode (see Figure 5). In the case of the other simulated neutron star spectra, a limited number of measured radii were 10% smaller (e.g., $0.6GM/c^2$) than the input value. This effect was only seen in simulations of spectra obtained with the EPIC-pn camera in "timing" mode. If these results are an accurate characterization of the systematic errors incurred when fitting mildly piled-up spectra with the EPIC-pn camera, it is a modest systematic error. Systematic uncertainties in the flux calibration between different cameras on the same observatory are approximately 7% (*XMM-Newton* calibration document XMM-SOC-CAL-TN-0083) and uncertainties between cameras on different missions can easily exceed 10% or more.
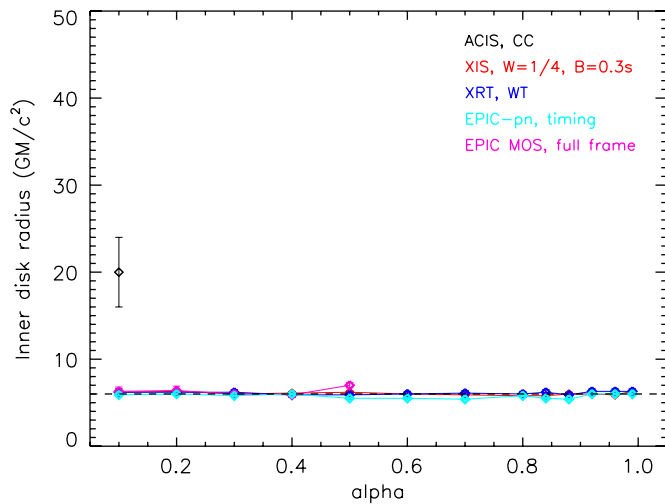
Figure 5. Evolution of the inner disk radius measured via a relativistic iron emission line (in units of GM/c^2) vs. the severity of photon pile-up (governed by the grade migration parameter α), for simulated spectra assuming a form typical of "Z" and "atoll" neutron star X-ray binaries (see Section 5 and Table 1). The dashed horizontal line marks the input radius of $6GM/c^2$. An iron line could not be required in fits to simulated *Chandra*/ACIS "continuous clocking" mode spectra past $\alpha = 0.1$. The results shown above suggest that other detectors and modes can deliver a nearly nominal response and accurate inner disk radii at the flux level assumed in our simulations.

(A color version of this figure is available in the online journal.)

The neutron star spectra that were simulated assuming a narrower and symmetric Gaussian emission line with $E = 6.7$ keV and $\sigma = 0.33$ keV (as per Ng et al. 2010) also give clear results. The Gaussian line width, line centroid energy, and the normalization of the disk blackbody component are plotted versus α in Figure 6. (The disk blackbody component is the lowest energy flux component in the spectral model, and changes to its flux trace the degree of flux redistribution due to photon pile-up.) When photon pile-up is modest, the line width and line energy are not strongly affected. At the flux levels simulated, the *XMM-Newton*/EPIC MOS "full frame" mode suffers more severe pile-up. The line becomes *narrower* as photon pile-up (traced by the grade migration parameter α) becomes more severe (see Figure 6). In no case do fits to the simulated spectra measure a line that is falsely broad, asymmetric, nor displaced to a significantly lower centroid energy. In short, narrower and symmetric lines are not observed to take on a relativistic shape due to photon pile-up distortions.

The result that pile-up generally tends to produce *falsely narrow* lines can largely be understood in simple terms. At high flux levels, photon pile-up will cause a CCD to register some low-energy events as having a higher energy. Photon pile-up adds to the high energy continuum. Adding extra flux in the Fe K band has the effect of hiding the true profile of a relativistic line: the red wing blends with the continuum and the (relatively) narrow blue wing is all that remains. The details of the input spectrum and the nature of a given CCD camera (its effective area curve, its effective frame time, how many event boxes tile an extraction region) are likely important. This may partially explain why slightly different results are obtained from simulated EPIC-pn "timing mode" spectra of neutron stars.

The trends seen in Figure 4 are generally observed whenever pile-up is important. A broad range of incident spectra peak at approximately 1.0–1.5 keV, as do many detector effective area curves. Pile-up of photons to twice that energy, combined with a typical drop in effective area at about 2 keV due abrupt
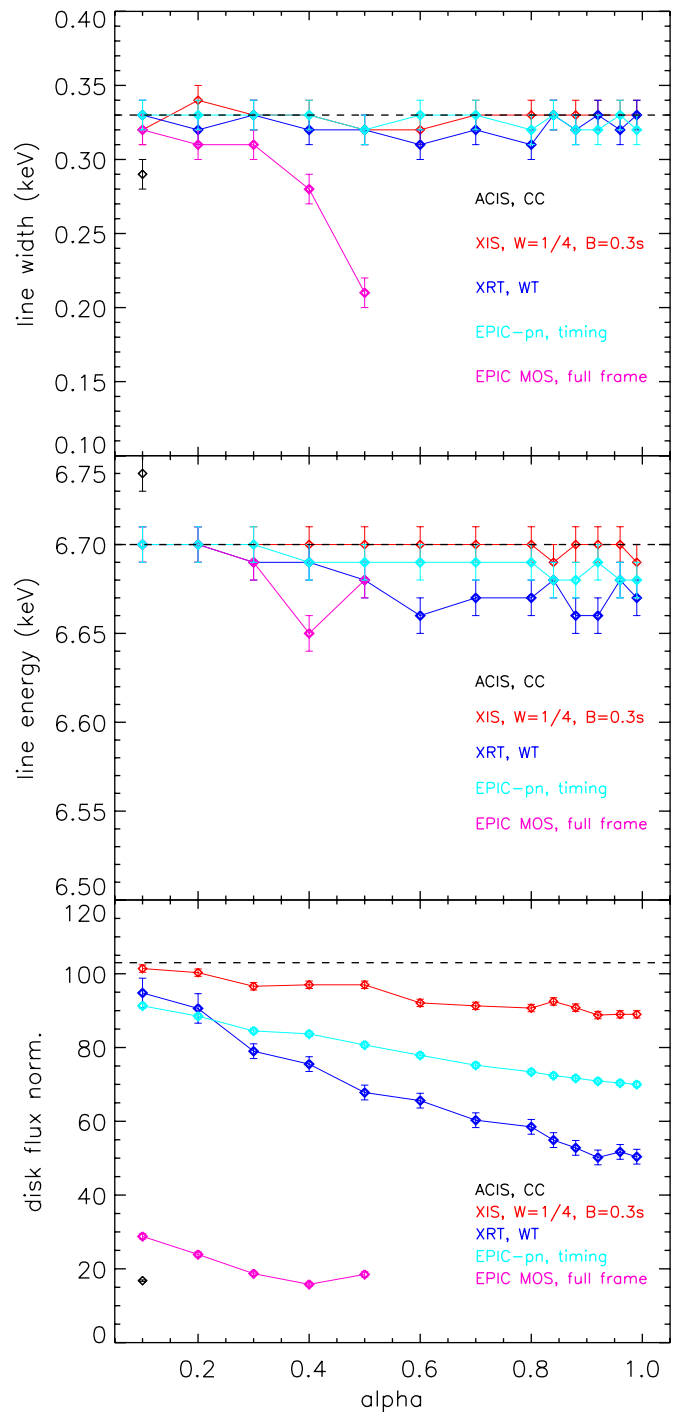
Figure 6. Results of replacing a relativistic line profile with a narrow Gaussian line (E=6.7 keV, $\sigma = 0.33$ keV) in simulated "Z" and "atoll" neutron star X-ray binary spectra. The line width (top), line energy (middle), and disk blackbody flux normalization (bottom) are plotted as a function of pile-up severity, as traced by the grade migration parameter α. Nominal input (simulated) values for each parameter are indicated by dashed horizontal lines (see Table 1). The disk blackbody is the lowest energy component in the spectral model, and the evolution of its flux normalization traces the degree of flux redistribution due to photon pile-up. The plots above clearly show that intrinsically narrow lines are not artificially broadened nor shifted to significantly lower energy by photon pile-up distortions. When pile-up is severe, intrinsically narrow lines are measured to be even narrower.

(A color version of this figure is available in the online journal.)

changes in the mirror reflectivity and also Si absorption in the CCD, causes a false excess in the 2–3 keV band. Depending on the specifics of the detector area curve, this excess may be
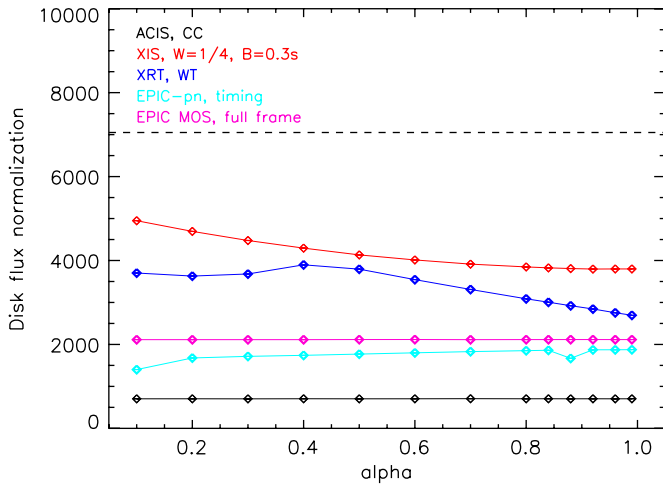
Figure 7. Evolution of the disk continuum flux normalization vs. the severity of photon pile-up (indicated by the grade migration parameter α), for simulated spectra assuming a form typical of the "high/soft" state in accreting black holes (see Section 5 and Table 1). The dashed horizontal line marks the input flux normalization level. The fact that the normalization is independent of α in the *XMM-Newton*/EPIC pn and MOS spectra and *Chandra*/ACIS spectra is an artifact of the simulations; it indicates that these modes are overwhelmed by the high flux typical of the "high/soft" state and none of these three modes should be regarded as better suited than the others in this regime. The flux levels indicated for these detectors and modes should not be regarded as realistic estimates of the flux decrement that would be observed. In contrast, the *Suzaku*/XIS (with a 1/4 window and 0.3 s burst option) and the *Swift*/XRT (in windowed timing mode) may be suited to this state but will give falsely small disk flux normalizations unless additional mitigations are taken. For the continuum model assumed, the disk radius is related to the square root of the disk normalization (e.g., measured normalizations that are a factor of 2–4 smaller than the simulated normalization indicate a radius that is too small by a factor of 1.4–2.0).

(A color version of this figure is available in the online journal.)

structured. Pile-up also adds appreciably through and above the Fe K band, causing the power law to be falsely hard and falsely high in flux. This is seen as a steadily increasing excess above 7 keV in the data/model ratio shown in Figure 4. The flux excess is greater when pile-up is more severe. When fit with typical spectral models, the flux excess at 2 keV–3 keV and above 7 keV act to create a false flux deficit just below the line energy, which is again more severe as pile-up becomes more severe. Owing to the fact that more flux redistribution occurs when pile-up is more severe, the full width of relativistic lines becomes increasingly difficult to measure accurately.

7.2. Pile-up and Disk Continua

As shown in Figure 7, severe photon pile-up can have a strong impact on efforts to study thermal emission from the accretion disk. Depending on the specific detector and the input flux level (again, traced by α), pile-up can falsely reduce the flux in the disk continuum by a factor of a few. The radius inferred from fits with the "diskbb" model depends on the square root of the flux normalization. More recent and physical disk models have more parameters, but still measure the flux to determine an innermost emission radius, and can be expected to be affected in the same degree. The results shown in Figure 7 depict the results of fits to simulated "high/soft" state spectra, but consistent results are also obtained in fits to the continuum in simulated spectra of other states (see the bottom panel in Figure 6).

This effect may also be understood relatively simply. Spectra of bright X-ray binaries tend to peak at or near to the peak of the effective area curve for X-ray telescopes with CCD spectrometers. This is typically also the energy range in which the

thermal disk continuum dominates. When pile-up is important, then, low energy flux is preferentially lost from the accretion disk component due to grade migration and flux redistribution.

It should be noted that even the baseline "high/soft" state flux levels are actually quite high (see Table 1). Simulations with successively higher values of the grade migration parameter α trace successively higher flux levels. Only the *Suzaku*/XIS with a 1/4 window and 0.3 s burst option, and the *Swift*/XRT in "windowed timing" mode, are even marginally able to cope with this flux level. Even for these detectors and modes, strong mitigations (e.g., annular extraction regions with large inner radii) would be required to recover accurate spectral parameters. The non-response of the other detectors and modes to increases in α (see Figure 7) merely indicates that the limits of the simulations are reached. The flux decrements indicated in Figure 7 for the *XMM-Newton*/EPIC MOS in "full frame" mode, EPIC-pn in "timing mode," and the *Chandra*/ACIS in "continuous clocking" mode, should not be taken as realistic estimates of observed flux decrements.

8. DISCUSSION

The results of the numerous simulations and fitting exercises detailed above suggest that severe photon pile-up affects relativistic disk spectra in clear and predictable ways.

Redistributing the low-energy continuum to the high-energy portion of the spectrum causes relativistic emission lines to become *falsely narrow*, giving a *falsely high* value for the inner disk radius. In turn, this means that estimates of black holes spin parameters based on the inner disk radius would be *falsely low*. In spectra where pile-up may be important and the success of mitigation is uncertain, emission lines give *upper limits* on the radius of the accretion disk, and *lower limits* on the value of the black hole spin parameter. The same trends are also observed in the case of neutron stars, both when relativistic and simple narrow Gaussian line functions are assumed.

Redistributing the low-energy continuum to the high-energy portion of the spectrum has exactly the opposite impact on disk continua. The modified disk continuum gives *falsely low* values of the inner disk radius, equating to *falsely high* values of black hole spin based on that radius. Therefore, when pile-up may be important, and/or when efforts to mitigate pile-up may not have been entirely successful, radii inferred from continuum fits are *lower limits* and inferred spin parameters are *upper limits*.

When two diagnostics are skewed in the same sense, it is difficult to detect a bias, and a potential check on derived quantities is lost. The results of the simple exercise undertaken in this paper are therefore fortuitous: photon pile-up distorts relativistic disk lines and the disk continuum in *opposing* ways. Fitting both lines and the disk continuum with relativistic spectral models and either checking that the radii agree, or explicitly requiring agreement in the fit (see Miller et al. 2009b), will help to derive results that are robust against pile-up distortions. This procedure may be more difficult in the case of neutron stars, however, because the disk continuum is typically less distinct in neutron star spectra.

Efforts to understand the inner accretion flow geometry through correlations between the flux in a disk line and the ionizing continuum are thus also impacted by photon pile-up. A particularly interesting explanation of the flux trends seen in Seyfert-1 AGN such as MCG-6-30-15 (Miniutti & Fabian 2004) and NGC 4051 (Ponti et al. 2006) is that gravitational light bending is altering the flux that impinges on the disk from a power-law source of ionizing radiation. In observations of

such sources, photon pile up *is not* a concern, but it might be a concern if CCD spectrometers were to monitor a stellar-mass accretor intensively. It is worth noting that current evidence of gravitational light bending in stellar-mass black holes is drawn from gas spectrometer data that is unaffected by pile-up (Miniutti & Fabian 2004; Rossi et al. 2005).

Two papers have recently commented on the possibility that photon pile-up might create falsely broad emission lines in black hole spectra. In the first example, *Suzaku*/XIS spectra of GX 339−4 in an "intermediate" state were extracted from different annuli and compared (Yamada et al. 2009). Spectra from larger annuli (presumably suffering from less pile-up) are not found to strongly require black hole spin. Yamada et al. (2009) suggest that pile-up may influence the line shape, but fitting results are consistent with a very broad line and a spinning black hole at the 90% level of confidence (see Miller et al. 2008). The relatively small number of counts in the wings of the PSF can partially account for the lack of a strong spin requirement and lower statistical certainty. A separate but equally important issue is that the disk reflection model used by Yamada et al. (2009) was not convolved with the line element expected for emission from the inner disk; this is physically inconsistent in that it implies a stationary, non-orbiting reflector. The immediate effect is to falsely add to the continuum in the vicinity of the emission line, falsely narrowing the line.

Recent work by Done & Diaz Trigo (2010) examined *XMM-Newton* spectra of GX 339−4 in a "low/hard" spectral state. Spectra from the MOS cameras were found to suffer from pile-up, even when extracting counts in annuli, whereas the EPIC-pn "timing" mode spectra were claimed to be free of distortions from photon pile-up. The pn spectra were also found to deliver narrower line profiles than the MOS spectra, implying a larger inner disk radius compared to values reported in prior work (e.g., Miller et al. 2004a; Reis et al. 2008; also see Wilkinson & Uttley 2009). Repeating the MOS extraction exactly as detailed in Reis et al. (2008), it is apparent that the disk line profile does not vary with the inner radius of annular extraction regions (see Figure 8). The line profile in the annulus identified by Done & Diaz Trigo (2010) as being largely free of pile-up, closely matches the line profiles seen in spectra extracted from smaller annuli, when each spectrum is allowed to have its own continuum. This means that the radii measured in the MOS spectra are not distorted by photon pile-up, but that the radii derived in fits to the pn spectra are distorted.

This conclusion is echoed by our simulations. The results detailed above strongly suggest that the fact of a narrower line profile in the pn means that it is actually piled-up and does not measure the true line width. Indeed, the departure of 2–3 GM/c^2 shown in Figure 2 is commensurate with the radius difference between fits to the MOS spectra reported by Miller et al. (2006) and Reis et al. (2008), and the pn spectrum as fit by Wilkinson & Uttley (2009). The data/model ratio in Figure 7 of Done & Diaz Trigo (2010) shows a flux excess at 2 keV and a flux decrement between 3 keV and the Fe K line, very similar to the trends shown in Figure 4 in this paper. The observed spectra and our simulation results both show that photon pile-up makes lines artificially narrow.

Following Done & Diaz Trigo (2010), Ng et al. (2010) have analyzed a number of spectra of neutron star low-mass X-ray binaries, observed with the *XMM-Newton*/EPIC-pn camera in "timing" mode. Their analysis suggests that the spectra suffer from a degree of photon pile-up. When the center of the PSF is excluded, the line profiles are found to be more consistent with
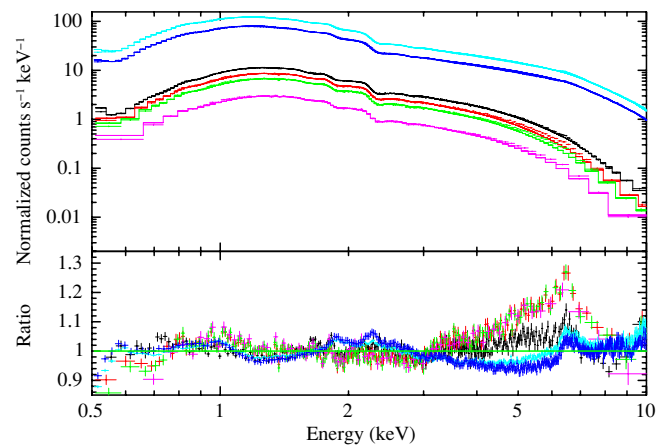
Figure 8. *XMM-Newton* MOS "full frame" and pn "timing" mode spectra of GX 339−4 (see Miller et al. 2006; Reis et al. 2008; and Done & Diaz Trigo 2010). Each spectrum was fit with a simple absorbed disk blackbody plus power-law model, ignoring the 4–7 keV band while fitting the continuum. The associated data/model ratios are shown in the bottom panel. The MOS spectra were extracted using inner exclusion radii of 0″ (black), 18″ (red), 25″ (green), and 50″ (yellow), and an outer radius of 120″ in all cases. In strong agreement with our simulations, the line profile in the black spectrum, which includes the piled-up core, is weaker and narrower than the line revealed in spectra extracted from annuli. The pn spectra were extracted using differing exclusion stripes, of 0″ (cyan), 20″.5 (magenta), and 49″.2 (blue). The data/model ratio for each pn spectrum reveals trends that match those found in our simulations of photon pile-up. However, the trends are not removed by excluding the center of the PSF, which argues against a strong pile-up contribution. Several other effects may also contribute to the pn residuals, including calibration uncertainties in the pn response function which become important at this high level of sensitivity.

(A color version of this figure is available in the online journal.)

Gaussian profiles. Ng et al. (2010) conclude that pile-up acted to falsely create skewed, relativistic line profiles. This conclusion runs counter to the results of our simulations, which show that (1) severe pile-up acts to falsely narrow both relativistic and simple Gaussian lines, not to falsely broaden lines; and (2) pile-up distortions to typical neutron star line spectra are not expected to be extreme (see Figure 5) for sources with flux levels similar to Serpens X-1, except for *Chandra*/ACIS "continuous clocking" mode.

Independent *Suzaku* and *XMM-Newton* observations of Serpens X-1 reveal relativistic Fe lines with a clear red wing (see Figure 9; also see Bhattacharyya & Strohmayer 2007, Cackett et al. 2008; Cackett et al. 2010). It is already clear that *Suzaku* line profiles in this source and similar sources do not depend on the inner radius of event extraction annuli (Cackett et al. 2010; see Figure 10)—the relativistic profiles do not result from photon pile-up. The nature of the line seen with *Suzaku* strongly suggests that the red wing seen in the *XMM-Newton* spectrum is due to dynamical broadening and red-shifting, not photon pile-up.

We re-reduced the *XMM-Newton* pn observation of Serpens X-1 exactly as detailed in Bhattacharyya & Strohmayer (2007), and extracted spectra including and excluding the center of the PSF. The primary effect of excluding the center of the PSF is merely to reduce the number of photons in the resultant spectrum, thereby lowering the sensitivity to the point that the red wing cannot be detected. The line is neither narrower nor weaker when the center of the PSF is excluded—it is simply less defined (see Figure 11). Ng et al. (2010) do not present direct comparisons of line profiles in spectra obtained in different extraction regions.

Given that (1) *Suzaku* spectra of neutron stars reveal relativistic lines that are clearly not due to photon pile-up distortions, (2)
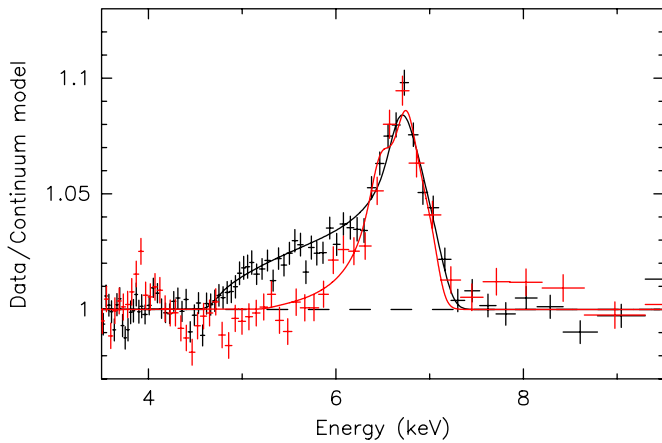
Figure 9. Relativistic line profiles detected in separate observations of the neutron star X-ray binary Serpens X-1 using *Suzaku* (black) and *XMM-Newton* (red). The line is broader in the *Suzaku* observation, though there is a clear red wing in the *XMM-Newton* line profile. (Figure adapted from a panel in Figure 9 of Cackett et al. (2010).)

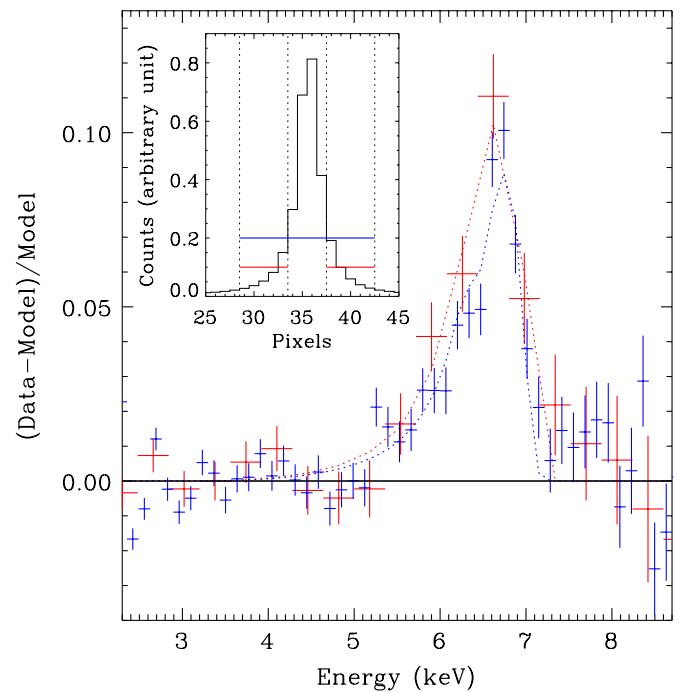(A color version of this figure is available in the online journal.)
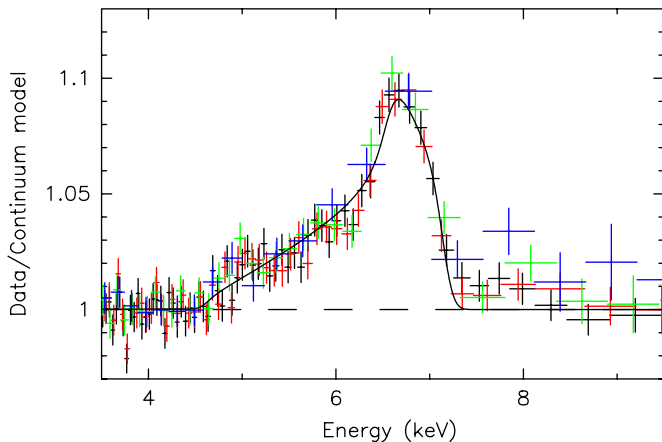
Figure 10. Relativistic line profile observed in Serpens X-1 with *Suzaku*. Photon pile-up can be checked and mitigated by extracting annular regions that avoid the center of the PSF. The different spectra shown above correspond to annuli of different inner exclusion radii: 0 pixels (black), 30 pixels (red), 60 pixels (green), and 90 pixels (blue). In this particular case, the line profile is clearly consistent in all spectra, indicating that pile-up in this spectrum is mild and does not affect the line profile significantly. (Figure adapted from Figure 2 in Cackett et al. 2010).

(A color version of this figure is available in the online journal.)

Figure 11. Relativistic line profile observed in Serpens X-1 with *XMM-Newton*. The blue data points and dotted model curve correspond to an extraction region including the center of the PSF. The red data points and dotted model line correspond to an extraction region that excludes the brightest central pixels. The inset figure displays the variation in the total counts extracted as a function of the extraction region. The relativistic profile of the line is evident in both spectra, and fully consistent. This strongly suggests that the relativistic line shape is *not* due to photon pile-up, and that excluding the center of the PSF results in a poorly defined line profile that is statistically more consistent with a Gaussian profile owing only to the reduced sensitivity of the spectrum.

(A color version of this figure is available in the online journal.)

a number of *Suzaku* and *XMM-Newton* line profiles are remarkably similar (e.g., SAX J1808.6−3808; see Figure 3 in Cackett et al. 2010; GX 349 + 2, see Figure 9 in Cackett et al. 2010), (3) the effect of excluding the center of the PSF in the *XMM-Newton* spectrum of Serpens X-1 is merely to reduce definition in the Fe line (not its width nor its strength), and (4) our simulations show that severe pile-up acts to artificially *narrow* both relativistic and simple Gaussian lines, it is likely that dramatic reductions in sensitivity drove the results obtained by Ng et al. (2010) and led to faulty conclusions regarding the ability of pile-up to create false relativistic line profiles.

The fact that sensitive spectra are required to detect the red wings of relativistic line profiles is not a revelation. This fact fueled the requirement of minimum sensitivity thresholds in recent surveys of relativistic lines in Seyfert AGN (see Nandra et al. 2007). Recent work on neutron star spectra makes the necessity of sensitive spectra even more clear. Deep

observations of a source such as GX 349+2 with *Suzaku* reveal a relativistic line profile, whereas short observations with the *Chandra*/HETGS—which has a lower collecting area—only recovers the narrower blue wing of the line profile (see Figure 3 in Cackett et al. 2009b). The *Chandra* spectrum is fully consistent with the relativistic line profile found using *Suzaku*; it simply does not have the sensitivity needed to detect the red wing against the continuum.

The above discussion is mostly focused on *XMM-Newton* and *Suzaku* spectroscopy, because the large effective area of these missions ensures that they are well suited to relativistic spectroscopy. *Swift* is highly flexible, but its smaller collecting area and short observations mean that typical spectra lack the sensitivity to detect and measure relativistic disk lines well. However, *Swift* is very well suited to black hole spin measurements using the disk continuum, and our results suggest that even in "windowed timing" mode, annular extraction regions are needed to avoid spectral distortions due to photon pile-up (see Figure 6). Brief discussions of pile-up and excluding the central portion of the PSF in "windowed timing" mode are given in Rykoff et al. (2007) and Rykoff et al. (2010).

Two combinations of detectors and modes are not treated in this work *because* they represent effective means of preventing photon pile-up. As noted previously, the "burst" mode of the EPIC-pn camera aboard *XMM-Newton* may provide the *best* means of preventing photon pile-up, as its short read-out time is suited to extremely bright sources. This comes at a cost in sensitivity, however, as "burst" mode has a live-time fraction

of just 0.03. Pile-up can also be avoided by observing with the *Chandra*/HETGS, which disperses a spectrum onto the ACIS spectrometer. Pile-up can be further avoided by reading-out the dispersed spectrum in "continuous clocking" mode.

Chandra/HETGS observations of the stellar-mass black hole GX 339−4 in an "intermediate" state measured an inner disk radius of $1.3^{+1.7}_{-0.1}\,GM/c^2$ (Miller et al. 2004b). This analysis used the same relativistically blurred reflection model applied to a later observation in the same state using *Suzaku* (Miller et al. 2008). Analysis of the later observation found a spin parameter of $a = 0.89 \pm 0.04$, corresponding to $r = 2.0 \pm 0.2 GM/c^2$ (Bardeen et al. 1972). The radius values measured in GX 339−4 are consistent in the two separate observations, using very different detectors. Similarly, *Chandra*/HETGS observations of the neutron star X-ray binary 4U 1705−44 find a very broad line, with a Gaussian width (FWHM) of 1.2 ± 0.2 keV; when fit with a relativistic diskline model, a radius of $r = 7^{+4}_{-1}\,GM/c^2$ is measured (Di Salvo et al. 2005). Here again, the line properties found using grating spectra—which avoid severe pile-up—are consistent with those found using *Suzaku* and *XMM-Newton* (Reis et al. et al. 2009; Di Salvo et al. 2009; Cackett et al. 2010), and inconsistent with the much narrower lines found by Ng et al. (2010) when extracting only the wings of *XMM-Newton*/EPIC-pn "timing" mode spectra. An *XMM-Newton*/EPIC-pn "burst" mode observation of GRS 1915 + 105 in a "plateau" state (similar to the low/hard state in most black holes) may also validate the results of our simulations and the discussion above. Martocchia et al. (2006) observed GRS 1915+105 twice in the "plateau" state—once in "timing" mode and once in "burst mode"—at consistent flux levels. The "timing" mode spectrum may suffer from modest distortions due to photon pile-up. The power-law index was measured to be harder than in the "burst" mode observation ($\Gamma = 1.686^{+0.008}_{-0.012}$ versus $\Gamma = 2.04^{+0.01}_{-0.02}$), indicative of possible pile-up. The iron line is found to be fairly narrow in the "timing" mode observation: the line is only visible above ∼6.2 keV when the spectrum is fit with a power law, the inner radius is constrained to be greater than $240 GM/c^2$, and a reflection fraction of $R = 0.35^{+0.02}_{-0.02}$ is measured. In contrast, when observed using "burst" mode, the line is visible down to 5 keV (or lower) relative to a simple continuum, a radius of less than $20 GM/c^2$ is required, and a reflection fraction of $R = 1.69^{+0.16}_{-0.04}$ is measured (Martocchia et al. 2006). (This *XMM-Newton*/EPIC-pn "burst" mode spectrum is broadly consistent with a *Suzaku* observation of GRS 1915+105 in the "plateau" state. In that spectrum, the line is also broad, and consistent with the ISCO; see Blum et al. 2009.) These results square with a central result of the simulations presented in this paper: photon pile-up acts to make relativistic lines appear to be falsely narrow.

Though an investigation is beyond the scope of this paper, it should be noted that efforts to mitigate pile-up can also distort spectra. The PSF of an X-ray telescope is energy dependent. Extracting events in annuli may avoid the piled-up core of a given PSF, but the spectrum is then derived from a portion of the PSF that is not calibrated as well as the core. Moreover, depending on the PSF, annular regions may only extract a vanishing fraction of the incident photon flux, complicating the detection of weak spectral lines. Relativistic disk lines are often 10%–20% features above the continuum; extracting spectra from regions of the PSF from which the energy and flux calibration are not known to much better than 10% could easily make it difficult to recover the details of a given line profile. Depending on how much flux is excluded in the annulus, limited

photon statistics will also serve to complicate the detection of line asymmetry.

Finally, it is worth emphasizing that our results depend on a specific combination of mirror technology and detector technology. Presently, CCD spectrometers sit at the focus of gold foil or gold-coated mirrors; this partially accounts for an overall telescope efficiency curve that is highest below 2 keV. New mirror technology, such as Si pore optics (e.g., Beijersbergen, M., et al., 2004), may produce different CCD photon pile-up effects, and distortions to disk continua and disk lines may not longer skew in the opposite sense.

9. CONCLUSIONS

Extensive simulations of photon pile-up for a number of spectral forms and detector parameters suggest that severe pile-up can distort spectroscopic signatures of the inner accretion disk, in largely predictable ways. The results of our work can be summarized as follows.

1. The degree of photon pile-up in a spectrum depends on the input flux level from a source and the effective area of the telescope, but it also depends on the number of event boxes tiling the PSF and the frame time of the CCD.
2. The relevant timescale for pile-up considerations is the time required to clock a full event box, not merely one row of charge.
3. Tiling the PSF with many event boxes and short frame times are two independent means of reducing photon pile-up. However, when short frame times are achieved by changing the size of an event box and undersampling the PSF, pile-up mitigation is partially compromised.
4. Flux redistribution due to photon pile-up causes emission lines—whether relativistic or symmetric and intrinsically narrow—to be observed as falsely narrow. Measured inner disk radii are then falsely large, and inferred black hole spin parameters are falsely low. Relevant observed spectra, though small in number, support this finding.
5. Grade migration due to photon pile-up causes the low-energy spectrum—principally the disk component—to have a falsely low flux. Measured inner disk radii are therefore falsely small and inferred spin parameters are falsely high.
6. Deriving inner disk radii and/or black hole spin parameters by linking that parameter to a joint value in both disk continuum and disk reflection models may yield more robust results when photon pile-up cannot be avoided or successfully mitigated.

REFERENCES

Arnaud, K. A. 1996, in ASP Conf. Series 101, Astronomical Data Analysis Software and Systems V, ed. G. Jacoby & J. Barnes (San Francisco, CA: ASP), 17
Ballet, J., et al. 1999, A&ASS, 135, 371
Bardeen, J. M., Press, W. H., & Teukolsky, S. A. 1972, ApJ, 178, 347
Barr, P., White, N. E., & Page, C. G. 1985, MNRAS, 216, 65
Beijersbergen, M., et al. 2004, Proc. SPIE, 5488, 868

Belloni, T., et al. 2005, A&A, 440, 207
Bhattacharyya, S., & Strohmayer, T. 2007, ApJ, 664, L103
Blum, J. L., et al. 2009, ApJ, 706, 60
Burrows, D. N., et al. 2005, Space Sci. Rev., 120, 165
Cackett, E. M., et al. 2008, ApJ, 674, 415
Cackett, E. M., et al. 2009a, ApJ, 694, L21
Cackett, E. M., et al. 2009b, ApJ, 690, 1847
Cackett, E. M., et al. 2010, ApJ, 720, 205
D'Aì, A., et al. 2009, ApJ, 693, L1
D'Aì, A., et al. 2010, A&A, 516, 36
Davis, J. E. 2001, ApJ, 562, 575
Davis, S. W., & Hubeny, I. 2006, ApJS, 164, 530
Di Salvo, T., et al. 2005, ApJ, 623, L121
Di Salvo, T., et al. 2009, MNRAS, 398, 2022
Done, C., & Diaz Trigo, M. 2010, MNRAS, 407, 2287
Dovciak, M., Karas, V., & Yaqoob, T. 2004, ApJS, 153, 205
Fabian, A. C., Rees, M. J., Stella, L., & White, N. E. 1989, MNRAS, 238, 729
Frank, J., King, A., & Raine, D. 2002, Accretion Power in Astrophyiscs (Cambridge: Cambridge Univ. Press)
Garmire, G., Bautz, M. W., Ford, P. G., Nousek, J. A., & Ricker, G. R. 2003, Proc. SPIE, 485, 28
George, I. M., & Fabian, A. C. 1991, MNRAS, 249, 352
Gorenstein, P., Gursky, H., & Garmire, G. 1968, ApJ, 153, 885
Haberl, F., et al. 2004, Proc. SPIE, 5165, 104
Hanke, M., et al. 2009, ApJ, 690, 330
Heinke, C. O. 2006, ApJ, 644, 1090
Hiemstra, B., et al. 2010, MNRAS, in press (arXiv:1004.4442)
Hill, J., et al. 2004, Proc. SPIE, 5165, 217
Jonker, P. G., et al. 2004, MNRAS, 351, 1359
Laor, A. 1991, ApJ, 376, L90
Li, L., et al. 2005, ApJS, 157, 335
Lin, D., Remillard, R. A., & Homan, J. 2007, ApJ, 667, 1073
London, R. A., Taam, R. E., & Howard, W. M. 1986, ApJ, 306, L170
Magdziarz, P., & Zdziarski, A. A. 1995, MNRAS, 273, 837
Makishima, K., et al. 1986, ApJ, 308, 635
Martocchia, A., et al. 2006, A&A, 448, 677
McClintock, J. E., et al. 2006, ApJ, 652, 518
Merloni, A., Fabian, A. C., & Ross, R. R. 2000, MNRAS, 313, 193
Miller, J. M. 2007, ARA&A, 45, 441
Miller, J. M., Cackett, E. M., & Reis, R. C. 2009a, ApJ, 707, L77
Miller, J. M., et al. 2002, ApJ, 578, 348
Miller, J. M., et al. 2003, MNRAS, 338, 7
Miller, J. M., et al. 2004a, ApJ, 606, L131
Miller, J. M., et al. 2004b, ApJ, 601, 450
Miller, J. M., et al. 2006, ApJ, 653, 525

Miller, J. M., et al. 2008, ApJ, 679, L113
Miller, J. M., et al. 2009b, ApJ, 697, 900
Miniutti, G., & Fabian, A. C. 2004, MNRAS, 349, 1435
Mitsuda, K., et al. 1984, PASJ, 36, 741
Nandra, K., O'Neill, P. M., George, I. M., & Reeves, J. N. 2007, MNRAS, 382, 194
Ng, C., Diaz Trigo, M., Cadolle Bel, M., & Migliari, S. 2010, A&A, in press
Nowak, M., Juett, A., Homan, J., Yao, Y., Wilms, J., Schulz, N. S., & Canizares, C. R. 2008, ApJ, 689, 1199
Papitto, A., et al. 2009, A&A, 493, L39
Park, S. Q., et al. 2004, ApJ, 610, 378
Ponti, G., et al. 2006, MNRAS, 368, 903
Reis, R. C., Fabian, A. C., & Miller, J. M. 2010, MNRAS, 402, 836
Reis, R. C., Fabian, A. C., & Young, A. J. 2009, MNRAS, 399, L1
Reis, R. C., et al. 2008, MNRAS, 387, 1489
Remillard, R., & McClintock, J. 2006, ARA&A, 44, 49
Revnivtsev, M., & Gilfanov, M. 2006, A&A, 453, 253
Reynolds, C. S., & Wilms, J. 2000, ApJ, 533, 821
Roberts, T. P., et al. 2004, MNRAS, 349, 1193
Ross, R. R., & Fabian, A. C. 2005, MNRAS, 358, 211
Rossi, S., Homan, J., Miller, J. M., & Belloni, T. 2005, MNRAS, 360, 763
Rykoff, E., Cackett, E., & Miller, J. M. 2010, ApJ, 719, 1993
Rykoff, E., Miller, J. M., Steeghs, D., & Torres, M. A. P. 2007, ApJ, 666, 1129
Shafee, R., et al. 2006, ApJ, 636, L113
Shakura, N. I., & Sunyaev, R. A. 1973, A&A, 86, 121
Shimura, T., & Takahara, F. 1995, ApJ, 445, 780
Sobczak, G. J., et al. 1999, ApJ, 520, 776
Sobczak, G. J., et al. 2000, ApJ, 544, 993
Struder, L., et al. 2001, A&A, 365, L18
Tanaka, Y., et al. 1995, Nature, 375, 659
Thorne, K. S. 1974, ApJ, 191, 507
Tomsick, J. A., et al. 2008, ApJ, 680, 593
Tomsick, J. A., et al. 2009, ApJ, 707, L87
Turner, M. J. L., et al. 2001, A&A, 365, L27
van der Woerd, H., White, N. E., & Kahn, S. M. 1989, ApJ, 344, 320
van Kerkwijk, M. H., et al. 2004, ApJ, 608, 432
Vaughan, S., & Fabian, A. C. 2004, MNRAS, 348, 1415
Wang, J., et al. 2010, ApJ, 714, 1497
Wilkinson, T., & Uttley, P. 2009, MNRAS, 397, 666
Wilms, J., Allen, A., & McCray, R. 2000, ApJ, 542, 914
Yamada, S., et al. 2009, ApJ, 707, L109
Zimmerman, E. R., Narayan, R., McClintock, J. E., & Miller, J. M. 2005, ApJ, 618, 832
Zhang, S. N., Cui, W., & Chen, W. 1997, ApJ, 482, L155